https://doi.org/10.5194/acp-2020-1075
Preprint. Discussion started: 16 November 2020

Atmospheric Chemistry and Physics Discussions

Structure, dynamics, and trace gases variability within the Asian summer monsoon anticyclone in extreme El Niño of 2015-16

Saginela Ravindra Babu[1,2 *], Madineni Venkat Ratnam[2], Ghouse Basha[2], Shantanu Kumar Pani[1] and Neng-Huei Lin[1,3*]

[1]Department of Atmospheric Sciences, National Central University, Taoyuan 32001, Taiwan

[2]National Atmospheric Research Laboratory, Gadanki 517112, India.

[3]Center for Environmental Monitoring and Technology, National Central University, Taoyuan 32001, Taiwan

*Correspondence to: S.R. Babu (baburavindra595@gmail.com) and N.-H. Lin (nhlin@cc.ncu.edu.tw)

Abstract: In this work, the detailed changes in the structure, dynamics and trace gases within the Asian summer monsoon anticyclone (ASMA) during extreme El Niño of 2015-16 is delineated by using Aura Microwave Limb Sounder (MLS) measurements, COSMIC Radio Occultation (RO) temperature, and NCEP reanalysis products. We have considered the individual months of July and August 2015 for the present study. The results show that the ASMA structure was quite different in 2015 as compared to the long-term (2005-2014) mean. In July, the spatial extension of the ASMA shows larger than the long-term mean in all the regions except over northeastern Asia, where, it exhibits a strong southward shift in its position. The ASMA splits into two and western Pacific mode is evident in August. Interestingly, the subtropical westerly jet (STJ) shifted southward from its normal position over northeastern Asia as resulted mid latitude air moved southward in 2015. Intense Rossby wave breaking events along with STJ are also found in July 2015. Due to these dynamical changes in the ASMA, pronounced changes in the ASMA tracers are noticed in 2015 compared to the long-term mean. A 30% (20%) decrease in carbon monoxide (water vapor) at 100 hPa is observed in July over most of the ASMA region, whereas in August

https://doi.org/10.5194/acp-2020-1075
Preprint. Discussion started: 16 November 2020

Atmospheric Chemistry and Physics Discussions

the drop is strongly concentrated in the edges of the ASMA. Prominent increase of O_3 (>40%) at 100 hPa is clearly evident within the ASMA in July, whereas in August the increase is strongly located (even at 121 hPa) over the western edges of the ASMA. Further, the temperature around the tropopause shows significant positive anomalies (~5K) within the ASMA in 2015. Overall, warming of the tropopause region due to the increased O_3 weakens the anticyclone and further supported the weaker ASMA in 2015 reported by previous studies.

Keywords: Trace gases, El Niño, Asian summer monsoon anticyclone, tropopause

1. Introduction

The Asian summer monsoon anticyclone (ASMA) is a distinct circulation system in the upper troposphere and lower stratosphere (UTLS) during northern hemisphere boreal summer and centered at ~25°N and extends roughly between 15°N to 40°N (Park et al., 2004; Randel et al., 2010). It is encircled by the subtropical westerly jet stream to the north and by the equatorial easterly jet to the south (Randel and Park, 2006). It is well recognized that the ASMA circulation is a prominent transport pathway for troposphere pollutants to enter the stratosphere (Randel et al., 2010). Previous studies have concluded that deep convection during summer monsoon can effectively transport the pollutants, aerosols and tropospheric tracers from the boundary layer into the UTLS region (Vogel et al., 2015; Santee et al., 2017;). These transported pollutants, tracers and aerosols become confined in the ASMA and, consequently, affect the trace gas composition in the UTLS region (Randerl et al., 2010; Solomon et al., 2010; Riese et al., 2012; Hossaini et al., 2015). It is clearly evident from the previous studies that the ASMA has a higher concentrations of tropospheric tracers such as carbon monoxide (CO), hydrogen cyanide (HCN) and Methane (CH_4) and lower concentrations of stratospheric tracers including Ozone (O_3) and nitric acid (HNO_3) (Park et al., 2004; Li et al., 2005; Park et al., 2008; Randel et al., 2010; Vernier et al., 2015; Yan

https://doi.org/10.5194/acp-2020-1075
Preprint. Discussion started: 16 November 2020

and Bian, 2015; Yu et al., 2017; Santee et al., 2017). The comprehensive study on the climatological composition in the ASMA can be found in Santee et al (2017). The ASM convection and orographic lifting are the primary mechanisms for the higher concentrations of the tropospheric tracers in the ASMA (Li et al., 2005; Park et al., 2007; Santee et al., 2017). Apart from these trace gases a strong persistent tropopause-level aerosol layer called as 'Asian Tropopause Aerosol Layer' (ATAL) also existed between 12 to 18 km within the ASMA and it was first detected from the CALIPSO measurements (Vernier et al., 2011).

Similarly, higher concentrations of water vapor (WV) within the ASMA during the summer monsoon is well documented in the literature (Gettelman et al., 2004; Park et al., 2007; Randel et al., 2010; Bian et al., 2012; Xu et al., 2014; Jiang et al., 2015; Das and Suneeth, 2020). Well known that the most of the water vapor enters the stratosphere through the tropical tropopause layer (Fueglistaler et al., 2009) and the temperature at the tropical tropopause controls the WV entering the lower stratosphere (LS). It is well documented that several processes such as convection, strength of the Brewer-Dobson circulation, El Niño–Southern Oscillation (ENSO) and Quasi-Biennial Oscillation (QBO) are responsible for the WV transport to the UTLS region (Holton et al., 1995; Jiang et al., 2010; Dessler et al., 2014; Jiang et al., 2015; Das and Suneeth, 2020). Khan and Jin (2016), studied the effect of gravity wave on the tropopause and WV in the Tibetan Plateau and reported that the gravity wave is the source for the WV transport from the lower to higher altitudes. The tropopause is higher within the ASMA during the summer monsoon period as compared the surrounding regions (Randel et al., 2010; Santee et al., 2017). Recently, Das and Suneeth (2020) reported about the causative mechanism for the presence of high WV in the ASMA region. The authors concluded that the UTLS water vapor in the ASMA is mainly controlled by the advection and tropopause altitude.

Convection during the summer monsoon is one of the major sources to transport the boundary layer pollutants into the UTLS region (Randel et al., 2010). It is well established that the ENSO has a strong influence on convection and circulation changes over the Asian monsoon region (Kumar et al., 1999; Wang et al., 2015; Gadgil and Francis, 2016). Enhanced (suppressed) convection over the Asian monsoon region generally observed in the cold phase of ENSO (warm phase of ENSO) known as La Niña (El Niño). Few studies have existed to date on the impact of ENSO on the ASMA trace gas composition changes and its dynamical changes. For example, Yan et al. (2018) reported the influence of ENSO on the ASMA with a major focus on how the ENSO winter signal propagates into the following seasons. They showed the weaker O_3 transport into the tropics during the onset of the ASMA after boreal winter El Niño events, but the difference between El Niño and La Niña composites becomes insignificant in the summer. In another study, Tweedy et al. (2018) demonstrated the impact of boreal summer ENSO events on O_3 composition within the ASMA in different phases of ENSO events. They reported that the ASMA forms earlier and stronger in the La Niña period that leads to greater equatorward transport of O_3-rich air from the extra-tropics into the northern tropics than during El Niño periods. Very recently, Fadnavis et al. (2019) reported higher concentrations of aerosol layers observed in the ATAL region during the El Niño period over the northern part of South Asia. However, the above- mentioned studies are mainly focused on changes in the ASMA with respect to ENSO on seasonal scales or mature stage of monsoon (combined mean of July and August) respectively.

Based on the above-mentioned studies, it is concluded that the ENSO also has a strong influence on the ASMA structure and its composition. The recent 2015-16 El Niño event was recorded as an extreme and long-lasting event in the 21st century (Huang et al., 2016; Avery et al., 2017). It was also one of the strongest El Niño events that occurred in the boreal summer (Tweedy

https://doi.org/10.5194/acp-2020-1075
Preprint. Discussion started: 16 November 2020

Atmospheric Chemistry and Physics Discussions

et al., 2018). In this event, several unusual changes occurred in the tropical UTLS region including, the strong enhancement in the lower stratosphere WV (higher positive tropopause temperature anomalies) over the Southeast Asia and western Pacific regions (Avery et al., 2017) and anomalous distribution of trace gases in the UTLS region (Diallo et al., 2018; Ravindra Babu et al., 2019). Similar way, the response of different trace gases (O3, HCl, WV) to the disrupted 2015–2016 quasi-biennial oscillation (QBO) associated with 2015-16 El Niño event is also reported by Tweedy et al. (2017). Dunkerton (2016), discussed the possible role of unusual warm ENSO event in 2015-2016 to the QBO disruption by triggering the extratropical planetary waves. Therefore, in the present study, we tried to investigate the detailed changes observed in the ASMA 2015 particularly focused on the structure, dynamics and trace gases variability within the ASMA in July and August 2015 by using satellite measurements and reanalysis products. The present research article is organized as follows. A database and methodology adopted are discussed in Section 2. The results and discussions are illustrated in Section 3. Finally, the summary and conclusions obtained from the present study are summarized in Section 4.

2. Database and Methodology

2.1. Microwave Limb Sounder (MLS) measurements

In the present study, version 4.2 Aura MLS measurements of CO, O_3 and WV are utilized. The MLS data of July and August months in each year from 2005 to 2015 period are considered. The vertical resolution for CO is in the range 3.5–5 km from the upper troposphere to the lower mesosphere and the useful range is 215–0.0046 hPa. The horizontal resolution for CO is about 460 km at 100 hPa and 690 km at 215 hPa. For WV, the vertical resolution is in the range of 2.0 to 3.7 km from 316 to 0.22 hPa and the along-track horizontal resolution varies from 210 to 360 km for pressure greater than 4.6 hPa. For O_3, the vertical resolution is ~2.5 km and the along-track

https://doi.org/10.5194/acp-2020-1075
Preprint. Discussion started: 16 November 2020

horizontal resolution varies between 300 and 450 km. The precision (systematic uncertainty) for WV is ~ 10-40% (~10-25%), for O_3 is ~0.02–0.04 (~0.02–0.05) ppmv and for CO, it is ~ 19 ppbv (30%), respectively. More details about the MLS version 4 level 2 data can be found in Livesey et al. (2018).

2.2. COSMIC Radio Occultation measurements

To see the changes in the tropopause temperature and height within the ASMA, we used high-resolution, post-processed products of level 2 dry temperature profiles obtained from Constellation Observing System for Meteorology, Ionosphere, and Climate (COSMIC) Radio Occultation (RO). Each month of July and August from 2006 to 2015 are considered. The data is downloaded from the COSMIC Data Analysis and Archival Center (CDAAC) website. We used 200 m vertical resolution temperature profiles in the study. Details of the temperature retrieval from the bending angle and refractivity profiles obtained from the RO sounding are presented well in the literature (Kursinski et al. 1997; Anthes et al. 2008). The COSMIC temperature have a precision of 0.1% between 8 and 25 km (Kishore et al. 2009; Kim and Son, 2012). The temperature accuracy in the UTLS is better than 0.5 K for individual profiles and ~0.1 K for averaged profiles (Hajj et al. 2004). It is noted that for individual RO temperature profiles, the observational uncertainty estimate is 0.7 K in the tropopause region, slightly decreasing into the troposphere and gradually increasing into the stratosphere (Scherllin-Pirscher et al., 2011a). For monthly zonal-averaged temperature fields, the total uncertainty estimate is smaller than 0.15 K in the UTLS (Scherllin-Pirscher et al., 2011b). Overall, the uncertainties of RO climatological fields are small compared to any other UTLS observing system for thermodynamic atmospheric variables. Note that these data are compared with a variety of techniques including GPS radiosonde data and observed good correlation particularly in the UTLS region (Rao et al. 2009; Kishore et al. 2009). The COSMIC

https://doi.org/10.5194/acp-2020-1075
Preprint. Discussion started: 16 November 2020

RO profiles have been widely used for studying the tropopause changes and its variabilities (Kim and Son, 2012; RavindraBabu et al. 2015; RavindraBabu et al. 2019b).

2.3. National Centers for Environmental Prediction (NCEP) data

We also utilized monthly mean Geopotential height (GPH) and wind vectors (zonal and meridional wind speed) from the National Centers for Environmental Prediction/National Center for Atmospheric Research (NCEP/NCAR) reanalysis (Kalnay et al., 1996), covering the same time period as the MLS observations (2005-2015). The horizontal resolution of NCEP/NCAR is 2.5° × 2.5°, respectively.

Apart from the above-mentioned data sets, we also used European Centre for Medium-Range Weather Forecasts (ECMWF) interim reanalysis potential vorticity (PV) data particularly at 350K isentropic surface in July and August 2015 (ERA-Interim; Uppala et al., 2005; Dee et al., 2011).

2.5. Methodology

Daily available MLS profiles of O_3, CO, and WV in each month are constructed and gridded by averaging the profiles inside bins with a resolution of 5° latitude × 5° longitudes. The following equation is used to estimate the relative change in percentage.

$$\text{Relative change in percentage} = \left(\frac{x_{i-\bar{x}}}{\bar{x}}\right) \times 100 \qquad (1)$$

where x_i represents the monthly mean of July/August in 2015, and $\bar{x}$ is the corresponding monthly long-term mean which is calculated by using the data from 2005 to 2014.

3. Results and Discussion

It is well reported that the ASMA is highly dynamic in nature with respect to its position and shape. Also it varies at different time scales i.e day-to-day, weekly and monthly scales caused by internal dynamical variability (Randel and Park, 2006; Garny and Randel, 2013; Pan et al., 2016; Nützel et al., 2016; Santee et al., 2017). The intensity and spatial extension of the ASMA are prominent

https://doi.org/10.5194/acp-2020-1075
Preprint. Discussion started: 16 November 2020

in July and August where the monsoon was in the mature phase (Santee et al., 2017; Basha et al., 2019). It can be noticed that the 2015-16 El Niño event was one of the strongest boreal summer events that occurred in the entire MLS data record (Tweedy et al., 2018). In this event, the Nino 3.4 data was exceeded +1.5 in July and +1.8 in August (**Fig. 1**). Therefore, in the present study, we mainly focused on ASMA behavior and trace gases changes in the ASMA on monthly scales particularly in July and August 2015 which represents strong El Niño.

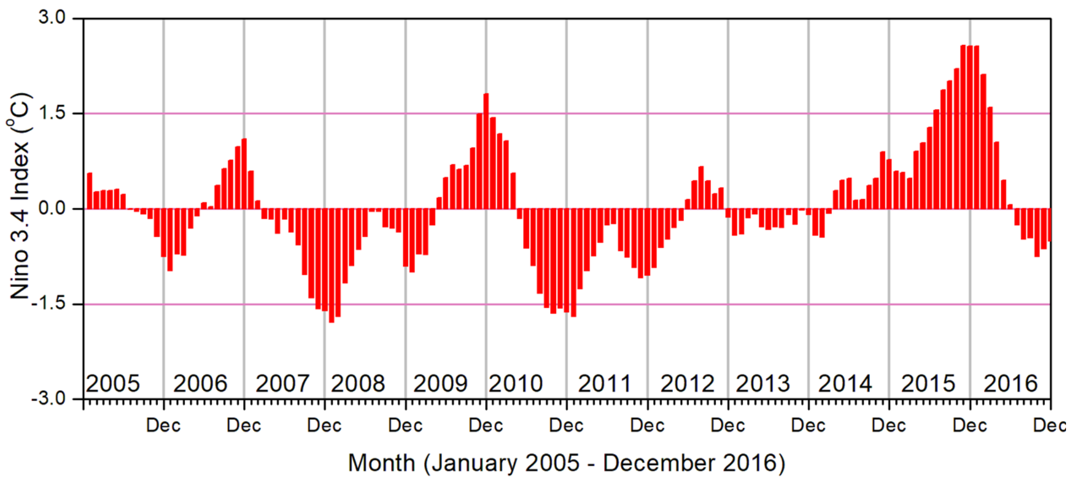

Figure 1. Temporal evolution of observed Niño3.4 Index data from January 2005 to December 2016.

3.1. Structure and dynamical changes in ASMA during 2015

In general, the studies looking at monthly or seasonal timescales related to the thermo-dynamical features in the ASMA, the anticyclone region is mostly defined from the simple constant GPH contours at different pressure levels (Randel and Park, 2006; Yan et al., 2011; Bergman et al., 2013; Basha et al., 2019). Previous researchers used different GPH contours at 100 hPa to define the anticyclone region. For example, Yan et al. (2011) used 16.7 km, Bergman et al. (2013) used 16.77 km and recently Basha et al. (2019) used 16.75 km GPH contour as the anticyclone region. Similar manner, we also defined the ASMA region based on NCEP reanalysis

https://doi.org/10.5194/acp-2020-1075
Preprint. Discussion started: 16 November 2020

GPH at 100 hPa and considered the 16.75 km GPH contour as the anticyclone region.

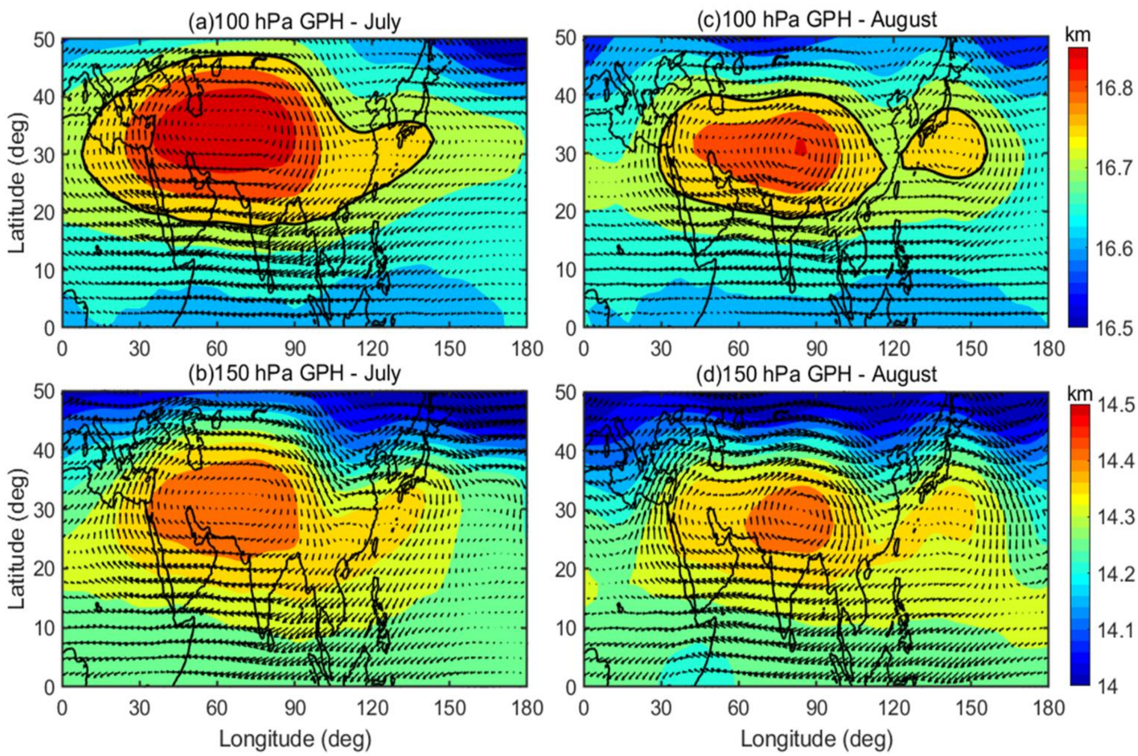

Figure 2. Spatial distribution of geopotential height observed in July 2015 (a) at 100 hPa and (b) 150 hPa superimposed with wind vectors at the respective corresponding levels. Subplots of (c) and (d) are the same as (a) and (b) but for the month of August. The black color solid contour lines represent the ASMA region at 100 hPa (16.75 km GPH contour).

The spatial distribution of GPH at 100 hPa and 150 hPa for the month of July (August) is shown in **Fig. 2a and 2b (Fig. 2c and 2d).** The corresponding monthly mean winds at respective pressure levels are also shown in **Fig.2**, respectively. The black solid line represents the ASMA region at 100 hPa based on 16.75 km GPH contour. The GPH distribution in **Fig. 2** shows clear distinct variability in the ASMA spatial structure between July and August at both pressure levels. For example, at 100 hPa, the maximum GPH center was located over western side in July whereas it was located over near to the Tibetan region in August. Interestingly the ASMA itself separated

https://doi.org/10.5194/acp-2020-1075
Preprint. Discussion started: 16 November 2020

Atmospheric Chemistry and Physics Discussions

into two anticyclones (16.75 km GPH contour black solid line in the figure) in August compare to July. The center of the small anticyclone was located over the northwestern pacific near 140^{o}E with the closed circulation indicated by the wind arrows.

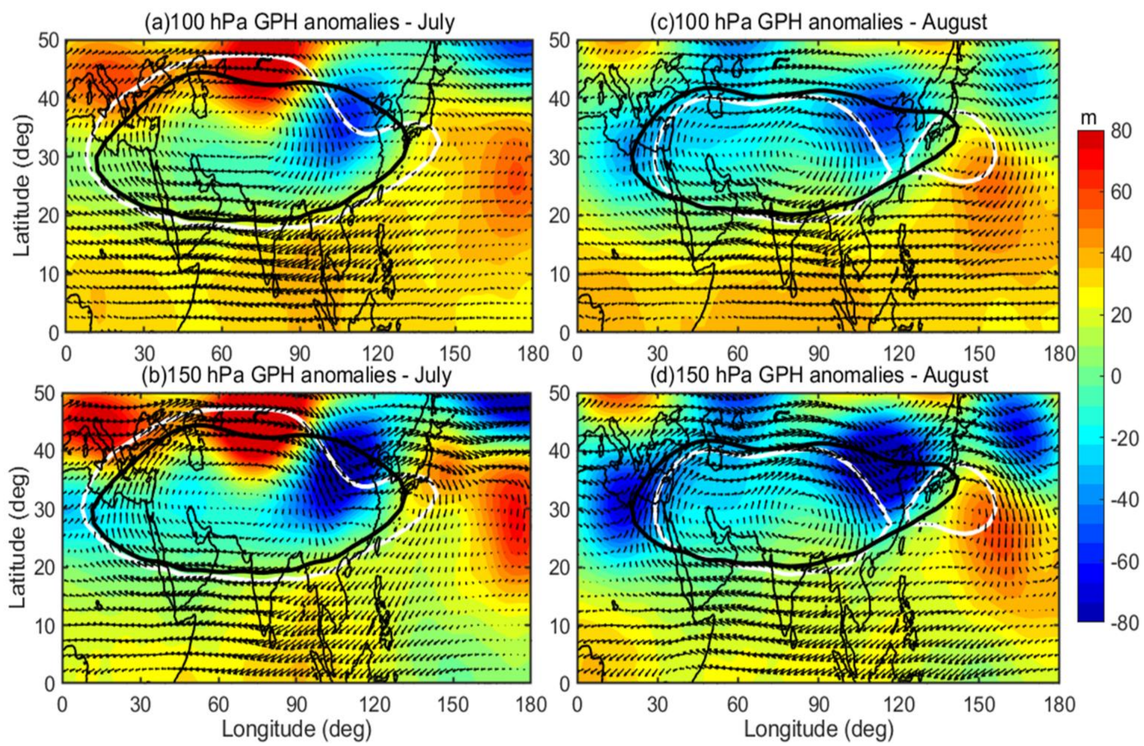

Figure 3. Spatial distribution of geopotential height anomalies observed in July 2015 (a) at 100 hPa and (b) 150 hPa superimposed with wind vectors at the respective corresponding levels. (c) and (d) same as (a) and (b) but for the month of August. The white color solid contour lines represent the ASMA region at 100 hPa (16.75 km GPH contour) observed in 2015 whereas the black color line represents the mean of 2005-2014.

Further, we compared the ASMA structure in 2015 with referenced long-term mean. For this, we obtained the GPH anomalies by subtracting the background long-term mean (2005-2014) from 2015. **Fig. 3** shows the latitude-longitudinal distribution of GPH anomalies (color shaded) along with wind vectors depicting circulation pattern at 100 hPa as well as at150 hPa during July and August. The white (black) color contour represents 16.75 km GPH at 100 hPa for the

https://doi.org/10.5194/acp-2020-1075
Preprint. Discussion started: 16 November 2020

corresponding month in 2015 (long-term mean). The GPH anomalies at both pressure levels show quite different features in July and August. A clear wave-like structures can be observed from the GPH anomalies. In July, the GPH anomalies exhibit strong negative maxima over 25-40^{o}N, 90-120^{o}E and positive maxima over 40-50^{o}N, 60-80^{o}E regions. The 16.75 km GPH contour lines in the ASMA region exhibits higher extension in all the directions except over the northeastern edges of the ASMA in July compared to the long-term mean. At the same location (northeastern edges), the ASMA exhibits a pronounced southward extension in July. Distinct features of GPH anomalies are noticed in August as compared to July. In August, the strong negative GPH anomalies are situated over the west and north-eastern edges of the ASMA.

It is well known that the subtropical westerly jet is an important characteristic feature of the ASMA (Ramaswamy 1958), and thus its changes during 2015 are also investigated. As the peak intensity of the westerly jet was located at 200 hPa (Chiang et al., 2015), we focused mainly on 200 hPa zonal wind changes in July and August. **Fig. 4a and 4c** (**Fig. 4b and 4d**) show the spatial distribution of long-term (2015) monthly mean zonal wind at 200 hPa during July and August. In general, the subtropical westerlies are located near to ~40^{o}N latitude during the mature phase of the monsoon period (Chiang et al., 2015). Compared to long-term mean, a significant weakening of the subtropical westerlies is noticed in 2015. Further, a strong southward shift in the westerlies is observed over the northeastern Asia region. This southward shift is moved even up to 30^{o}N in both months. From zonal wind at 200 hPa (**Fig. 4**) and wind vectors at 100/150 hPa (**Fig. 2**), it is clear that anomalous changes have occurred in the subtropical westerlies over the northeastern parts of the AMSA around 30-40^{o}N, 90-120^{o}E during July and August 2015. The southward shift in the westerlies is strongly associated with the southward extension of the ASMA over the northeastern side of the ASMA (**Fig. 2**). This is strongly supported by the previous

https://doi.org/10.5194/acp-2020-1075
Preprint. Discussion started: 16 November 2020

findings by Lin and Lu (2005) where they showed the southward extension of the South Asian High could lead to the southward shift of the westerly.

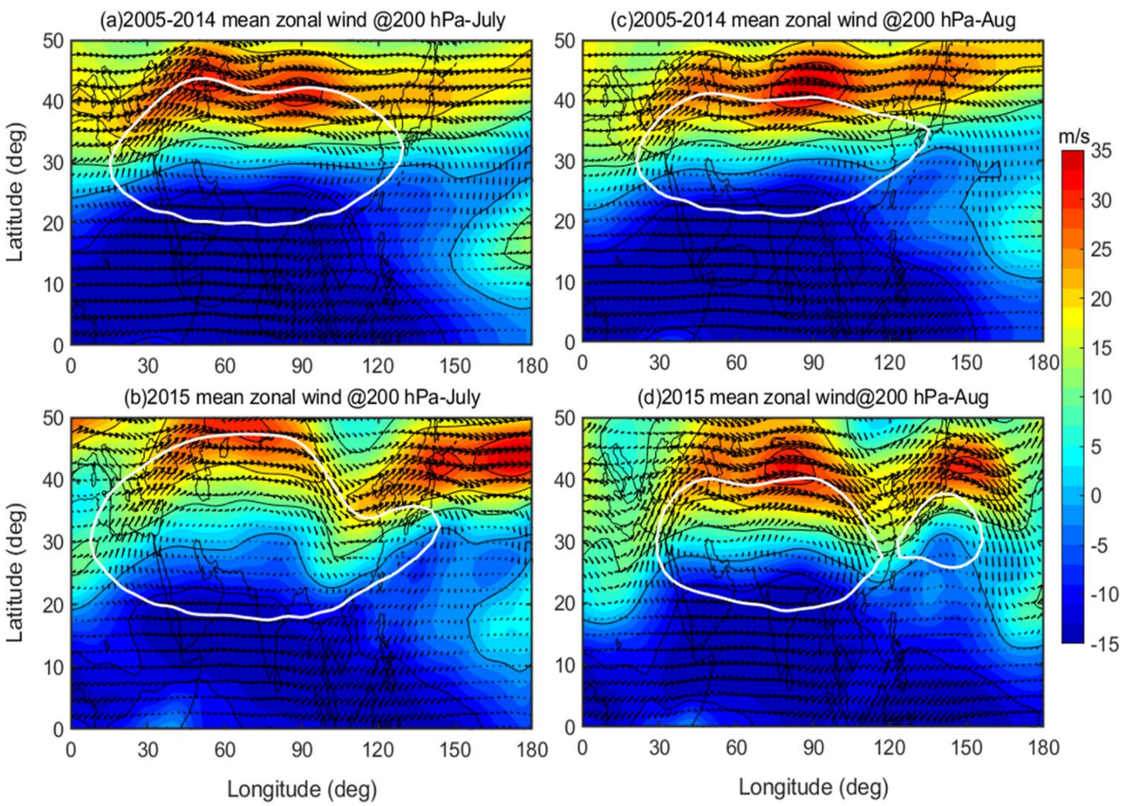

Figure 4. Spatial distribution of monthly mean zonal winds observed at 200 hPa in July during (a) 2005-2014 (b) 2015 year. (c) and (d) same as (a) and (b) but for the month of August. The white color solid contour lines represent the ASMA region at 100 hPa (16.75 km GPH contour).

From the GPH and winds observations, it is clear that pronounced changes are evident in the dynamical structure of the ASMA in 2015 and also relatively different features are noticed between July and August months. Interestingly the ASMA itself separated into two anticyclones during August 2015 and the separation exactly coincided with the strong negative GPH anomalies and southward meandering of subtropical westerlies over the northeastern side of the ASMA. The western pacific mode of the anticyclone is visible in August. The split of the anticyclone and the formation of the western Pacific (WP) mode are in agreement with previous studies reported by

https://doi.org/10.5194/acp-2020-1075
Preprint. Discussion started: 16 November 2020

few researchers earlier (e.g. Honomichl and Pan, 2020). The presence of the WP mode may be due to the eastward eddy shedding of the ASMA system in the process of its sub-seasonal zonal oscillation (Honomichl and Pan, 2020) or Rossby wave breaking (RWB) in the subtropical westerly jet (Fadnavis and Chattopadhyay, 2017). Fadnavis and Chattopadhyay (2017) also identified the split of ASMA into two anticyclones: one over Iran and another over the Tibetan region due to the RWB in June 2014 monsoon period. To see any signatures of these RWB in 2015, we further analyzed the RWB through the ERA interim reanalysis potential vorticity (PV) data. Based on previous studies, it is reported that RWBs can be identified from PV distribution at 350 K isentropic surface (Samanta et al. 2016; Fadnavis and Chattopadhyay, 2017). We used 350K isentropic surface PV data in July and August 2015 in the present analysis.

Figure 5a–b shows the distribution of ERA interim monthly mean PV at the 350 K isentropic surface during July and August 2015. It can be seen that, during July and August 2015, clear RWB signatures evident near 100^{o}E. It is noted that the equatorial advection of high PV values with a steep gradient and the southward movement of PV from the westerly jet are the basic features of the RBW (Vellore et al., 2016; Samanta et al. 2016). These features are clearly exhibited in **Figure 5** with higher PV values extends up to ~ 30^{o}N in both months over 100^{o}E region. The location of this RWB is significantly correlated with a southward meandering of westerlies and strong negative GPH anomalies. However, the observed RWB signatures in both months are from monthly mean PV data. Further, to see the clear signatures of these RWB, we made weekly based analysis for July month. For this we considered 1-7 July as week-1 and 8-14 July as week-2 so on. The weekly mean distribution of 350K isentropic surface PV during July is shown in **Figure 6**.

https://doi.org/10.5194/acp-2020-1075
Preprint. Discussion started: 16 November 2020

Atmospheric Chemistry and Physics
Discussions

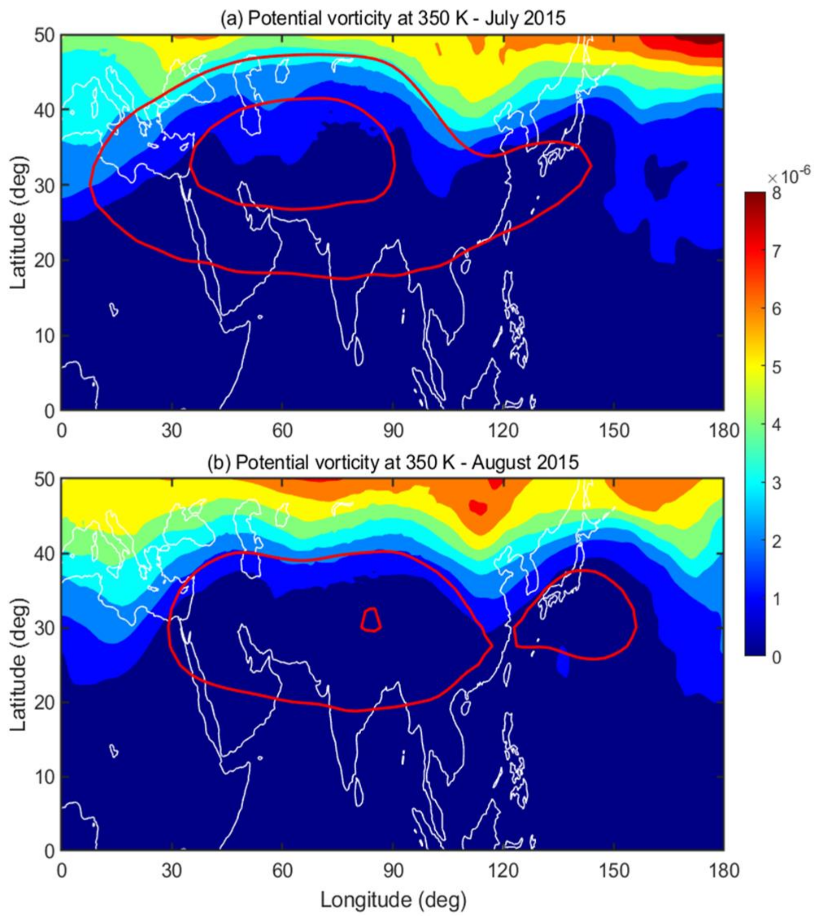

Figure 5. Distribution of potential vorticity (PV) on a 355 K isentropic surface in PVU (10-6 kg-im2s-2K): (a) monthly mean of July and (b) monthly mean of August 2015. Red color contours represent the anticyclone region during the respective months. The outer contour represents 16.75 km and the inner contour for 16.85 km geopotential height. Black arrows indicate the regions of RWB.

The black arrows in the figure represent RBW events during July 2015. At weekly scales, clear RWB signatures are observed over the anticyclone region. For example, in week-1 and week-2, the RWB signatures are evident over the northern region of the ASMA. However, in week-3 and week-4, these RWB signatures are very clear over northeastern Asia Even in week-5 (29July-04August), we noticed RWB signatures in PV data (Figure not shown). This clearly shows that

https://doi.org/10.5194/acp-2020-1075
Preprint. Discussion started: 16 November 2020

The RWB splits the ASMA into two anticyclones: one over the Tibetan region and another over the WP region. It is clear that the equatorward penetration of extra tropical forcing through the subtropical westerly jet is started in July and further amplified by the splitting of the ASMA into two during August.

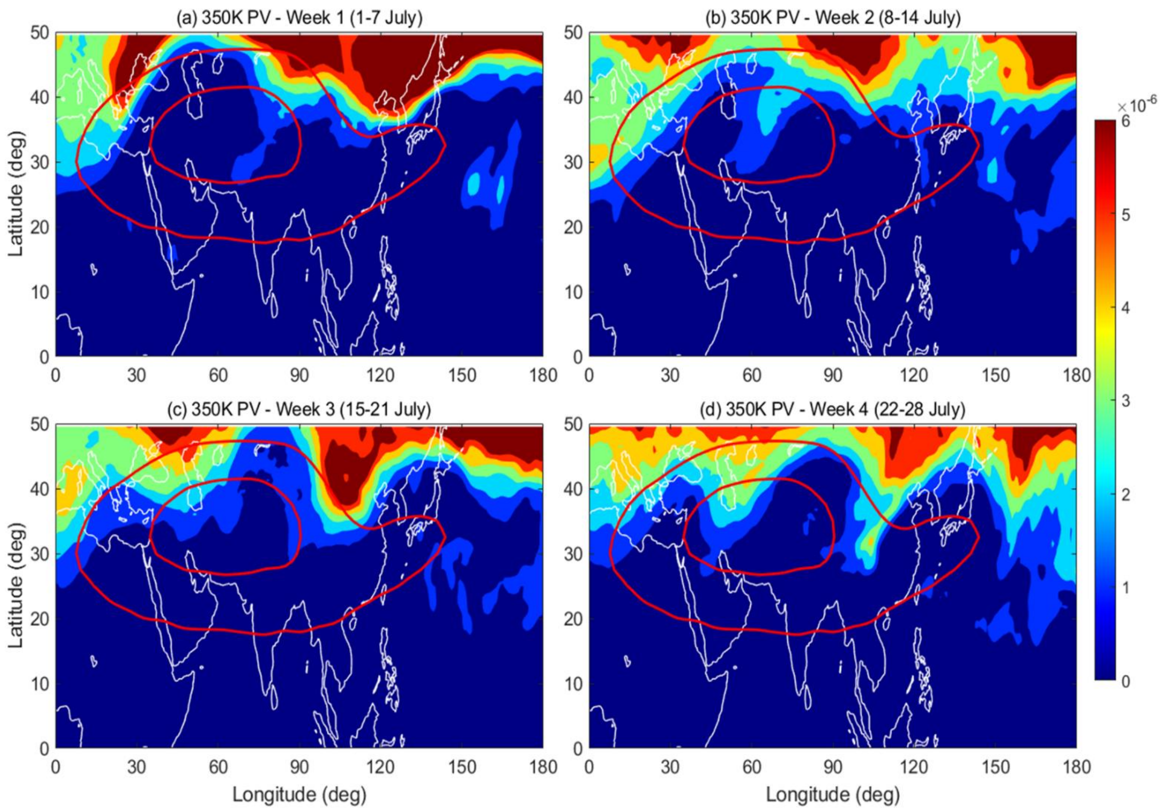

Figure 6. Same as **Figure 5**, but for the weekly distribution of PV in July 2015. Black arrows indicate the regions of RWB.

It is well known that the RWB is an important mechanism for horizontal transport between the extratropical lower stratosphere to the tropical UTLS region. These RWBs can act as an agent for the transport of extratropical stratospheric cold, dry, and O_3-rich air into the ASMA during the summer monsoon. Overall, it is concluded that the combination of the RWBs and strong southward meandering of the subtropical westerly jet in 2015 causes significant dynamical and structural

https://doi.org/10.5194/acp-2020-1075
Preprint. Discussion started: 16 November 2020

changes in the ASMA. These changes in the ASMA dynamical structure in 2015 can influence the concentrations of the different trace gases within the ASMA. Further we studied how much percentage change occurred in the O_3 concentration and other tropospheric tracers with in the ASMA during 2015 due to these dynamical changes. For this we extensively utilized MLS satellite trace gases measurements. The changes that occurred in the O_3 and CO, WV, are discussed in the following sections.

3.2. Trace gases anomalies observed within the ASMA in 2015

Well reported that the ASMA has low (high) concentrations of stratospheric tracers such as O_3 (tropospheric tracers such as CO, WV and etc.) and higher tropopause height compared to the region outside the ASMA during boreal summer (Park et al., 2007; Randel et al., 2010; Santee et al., 2017; Basha et al., 2019). Remarkable variabilities of these trace gases are attributed to the strong winds and closed streamlines associated with the ASMA, which act to isolate the air (Randel and Park 2006; Park et al. 2007). As mentioned in the introduction, the monsoon in 2015 was strongly affected by the strong El Niño conditions in July and August 2015. Based on the previous studies, the summer monsoon in 2015 was reported as a weaker monsoon and the ASMA circulation also relatively weak (Yuan et al., 2018; Tweedy et al., 2018). To see the changes in the trace gases during 2015, we generated the background long-term mean of CO, O_3, and WV by using 10 years of MLS trace gas data from 2005 to 2014. Here the results are discussed mainly based on the percentage change relative to the respective long-term monthly mean trace gases using **Equation 1**.

https://doi.org/10.5194/acp-2020-1075
Preprint. Discussion started: 16 November 2020

Atmospheric Chemistry and Physics
Discussions

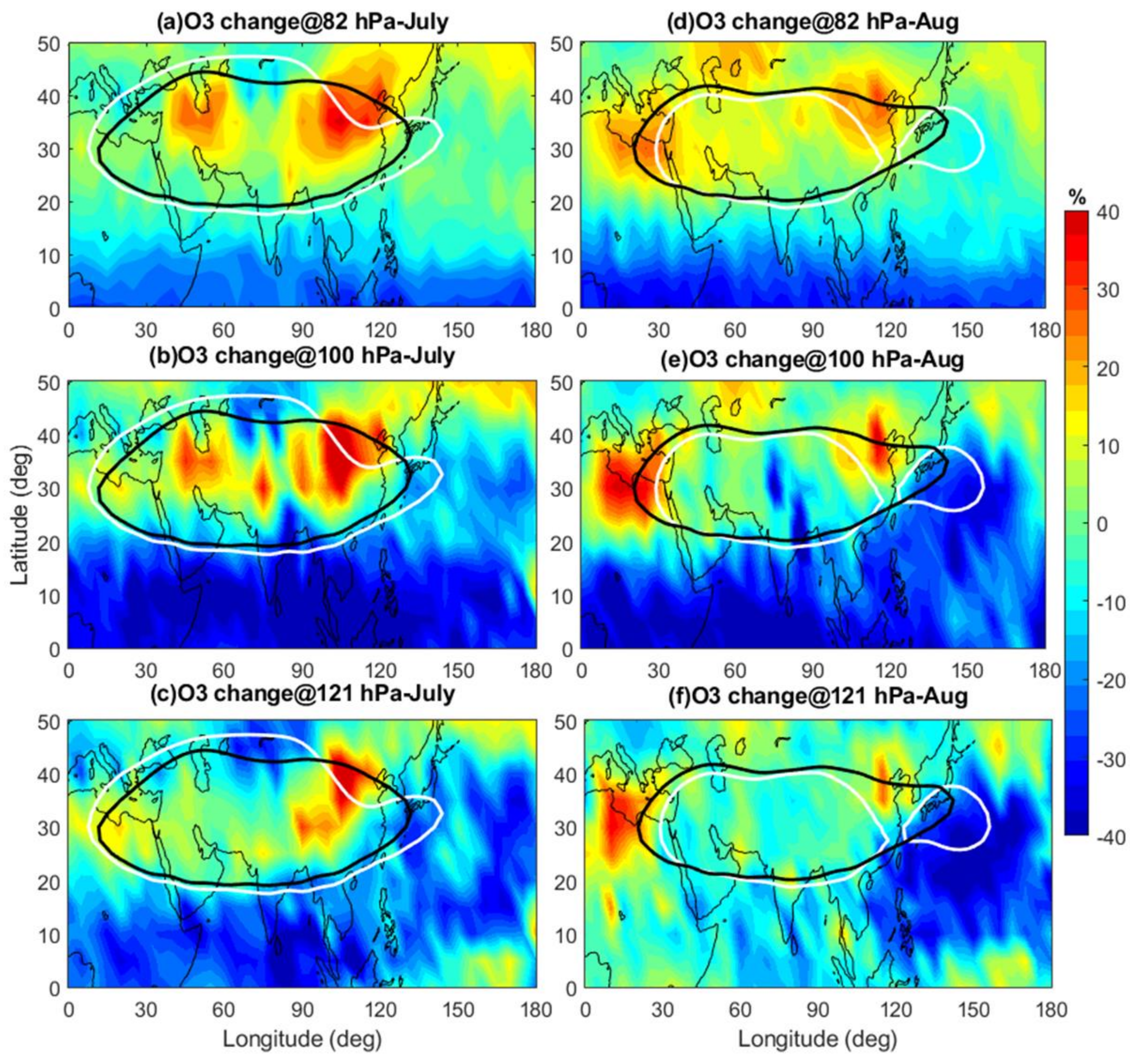

Figure 7. Ozone relative percentage change in July 2015 with respect to background climatological monthly mean observed at (a) 82 hPa, (b) 100 hPa and (c) 121 hPa. (c) and (d) same as (a) and (b) but for the month of August. The white (black) color contour represents 16.75 km geopotential height at 100 hPa for the corresponding month in 2015 (climatological).

Fig. 7a-c (**Fig. 7d-f**) show the distribution of relative percentage change in the O_3 concentrations in the anticyclone at 82 hPa, 100 hPa and 121 hPa during July (August) 2015. Distinct features are evident in the O_3 changes between July and August. Also, the observed changes in the O_3 are well correlated with the observed GPH anomalies in both months (**Fig. 3**).

In July, the O_3 shows a pronounced increase in the ASMA at all the pressure levels. This increase is quite significant over the northeastern edges of the ASMA and quite high at 100 hPa compared to 82 hPa and 121 hPa. A more than 40% increase is found at 100 hPa particularly over the northeastern edges of the ASMA in July. Even at 82 hPa and 121 hPa, significant enhancement in the O_3 concentrations are evident over the northeastern edges of the ASMA during July. This enhancement is clearly matching with the O_3 transport from higher latitudes which is shown in **Fig. 6** on a weekly scale from ERA interim data. Overall in July, the O_3 shows a prominent increase over the northeastern edges of the ASMA at all the mentioned pressure levels and strongly supported the stratosphere-troposphere transport over the same region. It can be noticed that the ASMA is strongly associated with troposphere-stratosphere transport as well as stratosphere-troposphere transport (Garny and Randel, 2016; Fan et al., 2017). Also it is well reported that the northern parts of the ASMA is an active region for stratosphere-troposphere transport processes (Sprenger et al., 2003; Škerlak et al., 2014).

In August, the O_3 shows quite different features compared to July. A strong increase in the O3 is observed over the western and eastern edges of the ASMA at all the pressure levels. The increase is quite significant at 100 hPa and even at 121 hPa. And the observed increase is found ~40% compared to the long-term mean at respective pressure levels. Even over the northeastern edges of the ASMA, the increase of O_3 still appeared in August as observed in July. It is noted that in July and August 2015, strong El Niño conditions have existed. We can expect a strong downwelling of the shallow branch of Brewer-Dobson circulation in the mid-latitudes (Diallo et al., 2018). Enhanced tropical upwelling over the tropics and strengthening of the downwelling in the northern hemisphere mid-latitudes are likely to cause for the observed higher O_3 in the northern mid-latitudes during El Niño. Due to the enhanced tropical upwelling, stronger ozone transport from

https://doi.org/10.5194/acp-2020-1075
Preprint. Discussion started: 16 November 2020

Atmospheric Chemistry and Physics Discussions

the tropics to the mid-latitudes is expected (Diallo et al., 2018). This clearly explains the observed high O_3 in the ASMA during 2015. Initially, during July, the O_3 is transported into the anticyclone from the northeastern edges of the ASMA region through the sub-tropical westerlies and then it is isolated within the ASMA region. This is further supported by the southward meandering of the westerly jet and southward shift of the ASMA (negative GPH anomalies) over the same region in July (**Fig. 3**). Also from the **Fig. 6**, very clear transport of mid latitude dry air into the ASMA through the intrusions is seen. Thus, it is clear from the results that the stratosphere to troposphere transport of O_3 along with the subtropical jet caused the strong enhancement of the O_3 within the ASMA in July 2015. The confined O_3 within the anticyclone during July further separated from the anticyclone and transported to the tropics as well as to the extra-tropics over the western edges of the ASMA (~30ºN) in August 2015.

Fig. 8a-b (**Fig. 8c-d**) shows the spatial distribution of CO relative percentage change at 100 hPa and 146 hPa observed in July (August) 2015. The white (black) color contour represents 16.75 km GPH at 100 hPa for the corresponding month in 2015 (climatological mean). The observed changes in the CO clearly exhibit quite distinct features between July and August. A significant decrease (~30%) is noticed in the CO concentrations over most of the AMSA in July. The maximum decrease of CO is noticed over the northeastern edges of the ASMA, located ~ 30-45ºN, 90-120ºE region. Whereas in August, the decrease of CO is more concentrated over the east and western edges of the ASMA at both the pressure levels. Overall, the MLS observed CO was ~30% below average (percentage decrease) compared to the climatological monthly mean within the ASMA in July and edges of the ASMA in August 2015.

https://doi.org/10.5194/acp-2020-1075
Preprint. Discussion started: 16 November 2020

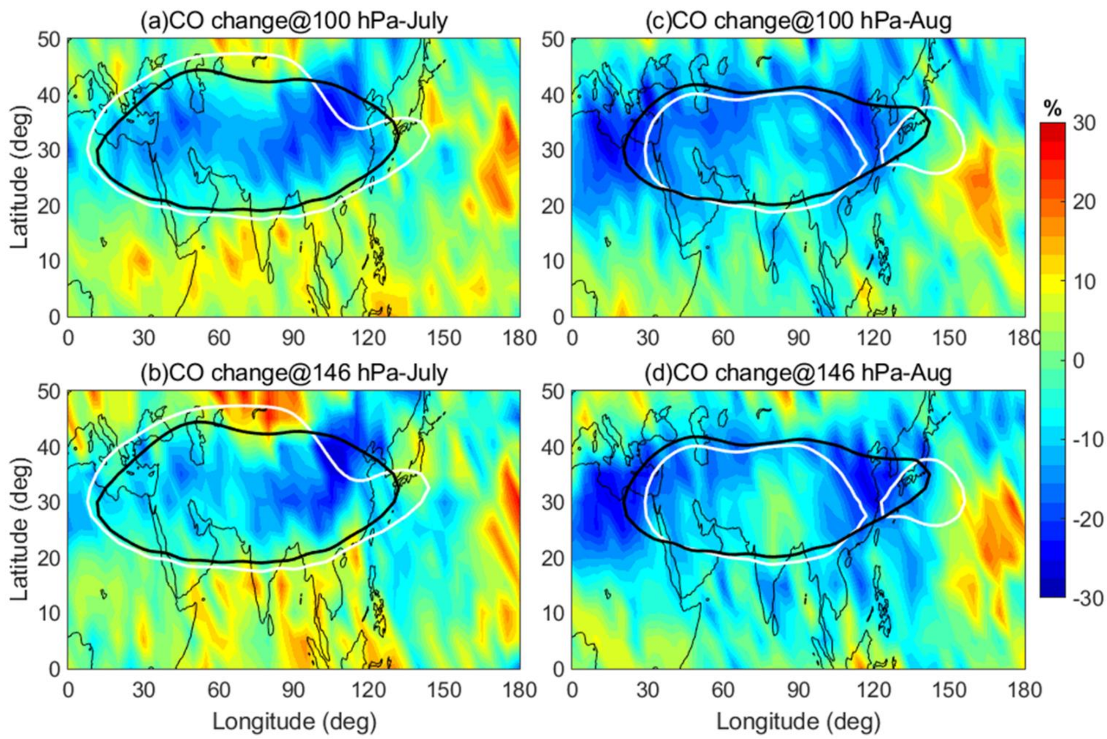

Figure 8. Carbon monoxide relative percentage change in July 2015 with respect to climatological monthly mean observed at (a) 100 hPa and (b) 146 hPa. (c) and (d) same as (a) and (b) but for the month of August.

Similarly, the WV relative percentage change at 100 hPa and 146 hPa in July (August) 2015 are shown in **Fig. 9a-b** (**Fig. 9c-d**). The WV shows quite different changes at both the pressure levels in July and August. At 146 hPa, the WV exhibits a strong decrease (> 20%) within the ASMA in July as well as in August also. However, at 100 hPa, the WV shows a relatively significant decrease within the ASMA in July compared to August. From the WV observations, it is concluded that the WV is strongly decreased at 146 hPa in both months. Whereas at 100 hPa, the decrease in WV is quite high in July compared to August. Overall, the tropospheric tracers (CO and WV) significantly decreased (~30% and 20%) within the ASMA during July and August 2015. These changes in the tropospheric tracers are might be due to the weaker vertical motions during the 2015

https://doi.org/10.5194/acp-2020-1075
Preprint. Discussion started: 16 November 2020

monsoon. Well reported that the summer monsoon in 2015 was weaker monsoon due to the strongest El Niño conditions existed in 2015 (Tweedy et al., 2018; Fadnavis et al., 2019). These El Niño conditions will suppress the monsoon convection and cause weaker vertical transport during monsoon.

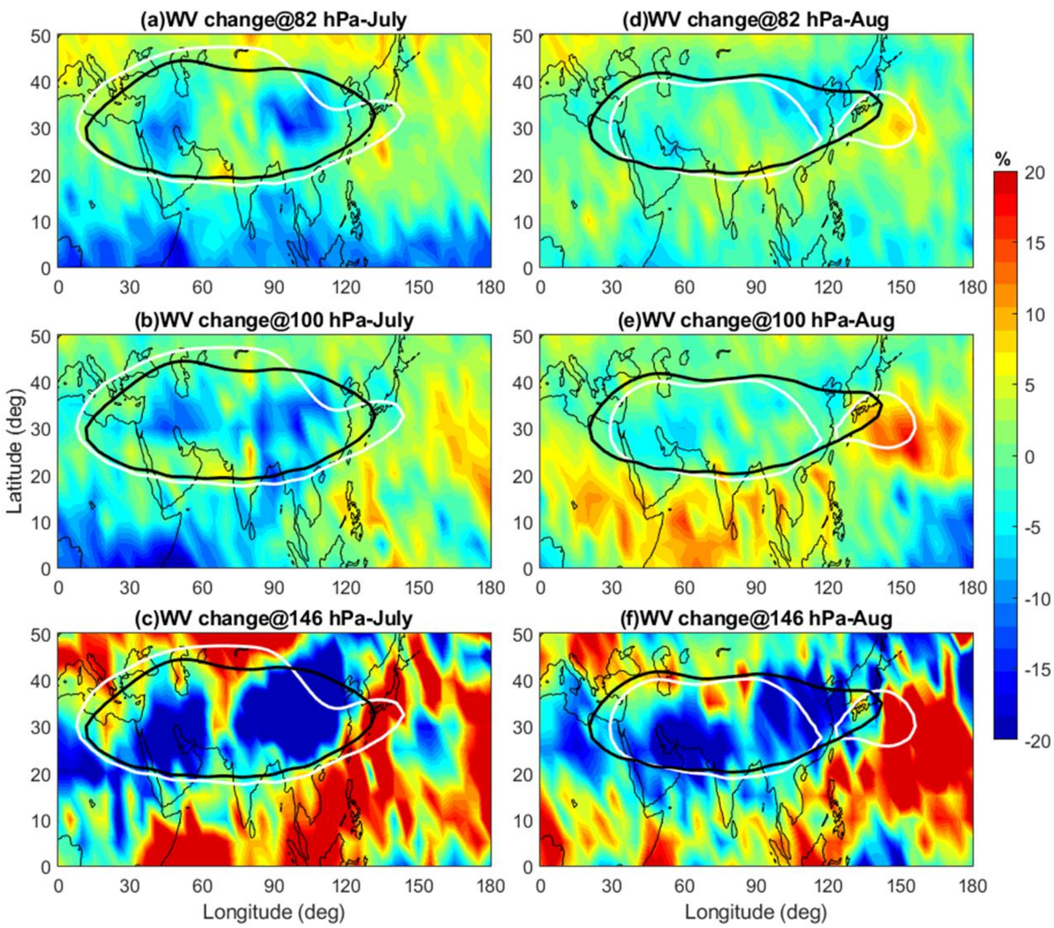

Figure 9. Water vapour relative percentage change in July 2015 with respect to background climatological monthly mean observed at (a) 82 hPa, (b) 100 hPa and (c) 146 hPa. (c) and (d) same as (a) and (b) but for the month of August.

From these results, it is clear that the enhancement of O_3 and lowering of CO/WV is evident in July and August 2015 compared to the climatological monthly mean. The observed high O_3 and low WV from the present study are consistent and well-matched with the previous study reported by Li et al. (2018). They demonstrated the importance of the large-scale atmospheric dynamics and the stratospheric intrusions for high O_3 and low WV over Lhasa within the ASMA by using in-situ balloon-borne measurements. The O_3/WV changes strongly influence the background temperature structure within the UTLS region (Ratnam et al., 2016). Further, we tried to investigate the tropopause temperature changes within the ASMA by using COSMIC RO data. The results are presented in the next following section.

3.3. Tropopause temperature anomalies in 2015

It is a well-known feature that the tropopause is higher over the ASMA than the surrounding regions (Randel et al., 2010; Santee et al., 2017). Also well documented that most of the STE processes that include WV and O_3 transport between troposphere and stratosphere are occur through the tropopause (Fueglistaler et al., 2009; Ratnam et al., 2016; Ravindra Babu et al., 2015, 2019b, 2020). In the present study, we mainly focused on changes in the cold point tropopause temperature (CPT) and lapse rate tropopause temperature (LRT) within the ASMA in July and August 2015. The July and August 2015 monthly mean tropopause parameters are removed from the respective climatological monthly mean which is calculated by using COSMIC RO data from 2006 to 2014. Kindly noticed that the analysis is strictly restricted within the 45° N region for the cold point tropopause. **Fig. 10a-b** (**Fig. 10c-d**) show the CPT and LRT anomalies observed in July (August) 2015. The tropopause temperature anomalies (CPT/LRT) also exhibit a distinct pattern in July and August as observed in O_3 (**Fig. 7**). In July, the CPT/LRT anomalies show strong positive anomalies (~5 K) in most of the ASMA region. High positive CPT/LRT anomalies are also noticed over the northwestern pacific (NWP) region particularly below 20°N. These CPT/LRT anomalies observed over the NWP region are might be due to the El Niño induced changes in the Walker

https://doi.org/10.5194/acp-2020-1075
Preprint. Discussion started: 16 November 2020

circulation. Previous studies also observed significant warm tropopause temperature anomalies over WP and maritime continent during the El Niño period (Gettlemen et al., 2001). In August, the strong positive CPT/LRT anomalies (~5K) are concentrated over the northeastern edges of the anticyclone where the western pacific mode of the anticyclone is separated from the ASMA. The temperature anomalies at 1 km above and below the CPH also show similar behavior as seen in the CPT/LRT during August 2015. Overall, the tropopause temperature anomalies in July and August 2015 within the ASMA well correlated with the strong enhancement in the O_3 as shown in **Fig. 7.** It is concluded that the enhanced O_3 within the ASMA is a main possible reason for the observed strong positive tropopause temperature anomalies in July and August 2015.

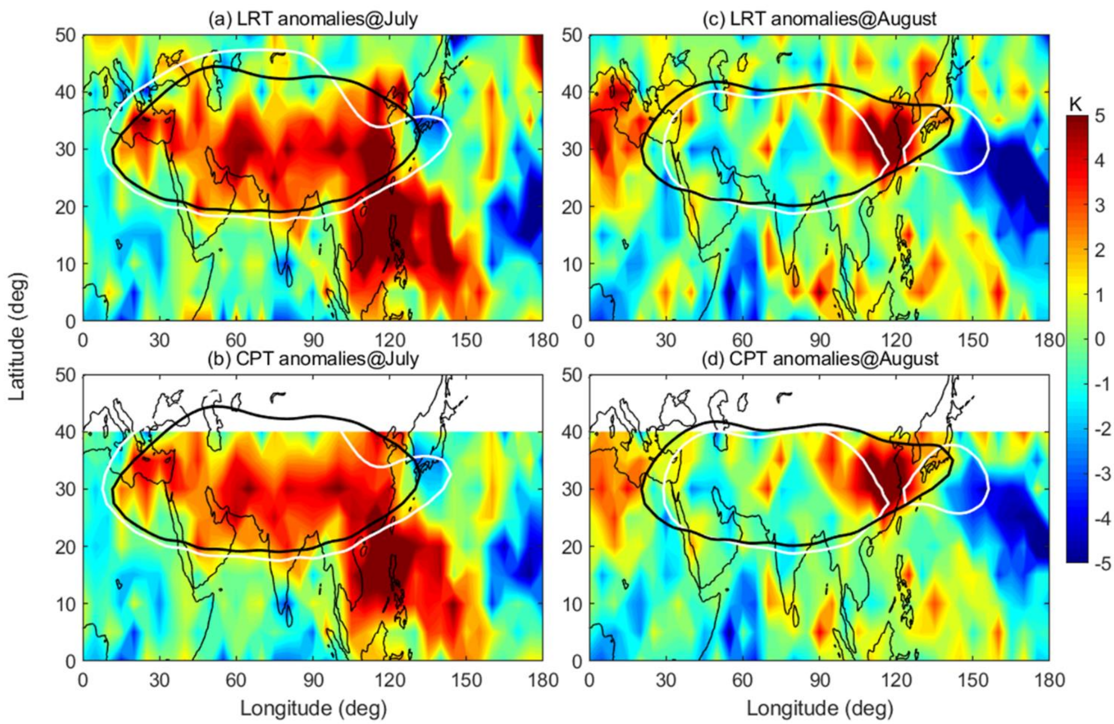

Figure 10. Spatial distribution of (a) lapse rate tropopause temperature (LRT), (b) cold point tropopause temperature (CPT) anomalies in July 2015. (c) and (d) same as (a) and (b) but for the month of August 2015. The white (black) color contour represents 16.75 km geopotential height at 100 hPa for the corresponding month in 2015 (climatological).

https://doi.org/10.5194/acp-2020-1075
Preprint. Discussion started: 16 November 2020

4. Summary and Conclusions

In this study, we investigated the detailed changes observed in the structure, dynamics and trace gases (Ozone, Water Vapor, Carbon Monoxide) variability within the ASMA in 2015 by using reanalysis products and satellite measurements. The tropopause temperature (CPT and LRT) on monthly scales particularly during July and August 2015 also discussed. To quantify the changes that happened within the ASMA region, 11 years (2005-2015) of O_3, WV and CO observations from the Aura-MLS data and 10 years (2006-2015) of tropopause temperature data from the COSMIC RO temperature profiles are used. The NCEP reanalysis observed winds and GPH data from 2005 to 2015 are also utilized. The results are obtained by comparing the trace gas quantities in July and August 2015 with corresponding long-term monthly mean quantities.

The trace gases within the ASMA exhibit substantial anomalous behavior in July and August 2015. During July and August 2015, we observed an enhancement of O_3 and the lowering of CO and WV over most of the ASMA region. The decrease of the tropospheric tracers (CO and WV) is quite expected due to the weaker upward motions from the weak monsoon circulation in 2015. This is supported by a recent study reported by Fadnavis et al. (2019). They showed weaker upward motions and deficient rainfall in the 2015 monsoon due to the strong El Niño conditions. However, the strong enhancement in the stratospheric tracer (O_3) over within the ASMA particularly over the northeastern edges of the ASMA during July is quite interesting. This is might be due to the stratospheric intrusions as well as transport from the mid-latitudes. Based on Fishman and Seiler (1983), it was stated that the positive correlation between CO and O_3 indicates, the O_3 is produced by in-situ in the troposphere whereas the correlation is negative means the O_3 originates from the stratosphere. We noticed a strong negative correlation between CO and O_3 in the present study with increased O_3 and decreased CO from the MLS measurements. This clearly reveals that the

https://doi.org/10.5194/acp-2020-1075
Preprint. Discussion started: 16 November 2020

observed increased O_3 within the ASMA during 2015 is the stratospheric origin. This is further supported by higher negative GPH anomalies associated with a southward meandering of the subtropical westerly jet over northeastern Asia in July (**Fig. 3** and **4**). Further, the increased O_3 at 100 hPa and 121 hPa over western edges of the ASMA during August clearly indicates the transport of the O_3 towards outer regions through the outflow of the ASMA (**Fig. 7e-f**). Interestingly, the tropopause temperature obtained from the COSMIC RO data in July 2015 shows strong positive temperature anomalies (~5 K) over the entire ASMA region. These warm tropopause temperatures again supported the increased O_3 within the ASMA during 2015. The major findings obtained from the present study are summarized in the following.

- ❖ The spatial extension of the ASMA region shows higher than long-term mean except over northeastern Asia where it exhibits a strong southward shift in July. Whereas in August, the AMSA further separated into two anticyclones and the western Pacific mode anticyclone is clearly evident in August.
- ❖ The combination of Rossby wave breaking and pronounced southward meandering of subtropical westerlies play a crucial role on the dynamical and structural changes in the ASMA in 2015.
- ❖ Strong enhancement in O_3 at 100 hPa (>40%) is clearly evident within the ASMA and particularly higher over the northeastern edges of the ASMA in July. The enhanced O_3 is strongly associated with a dominant southward meandering of the subtropical westerlies. In August, the increased O_3 is significantly located over the western edges of the ASMA. This clearly indicates the transport from the ASMA to the edges through its outflow.
- ❖ A 30% (20%) decrease in CO (WV) is observed within the ASMA in 2015. The decrease in the WV is higher at 146 hPa than 100 hPa.

https://doi.org/10.5194/acp-2020-1075
Preprint. Discussion started: 16 November 2020

- ❖ Significant positive tropopause temperature anomalies (~5 K) is observed in the entire ASMA region in July whereas, in August, the strong positive anomalies are concentrated over the northeastern side of the ASMA.

The changes in the O_3 concentrations (increase/decrease) within the ASMA are one of the possible mechanisms to strengthening/weakening of the ASMA (Braesicke et al., 2011). By using idealized climate model experiments, Braesicke et al. (2011) demonstrated that the strengthening (weakening) of the ASMA occurred when the O_3 is decreased (increased) within the ASMA. The increased O_3 within the ASMA warms the entire anticyclone region and weakens the ASMA. By using precipitation index, wind data and stream functions, previous studies reported that the ASMA circulation in 2015 was weaker than the normal (Tweedy et al., 2018; Yuan et al., 2018). Based on our present results, we conclude that the strong enhanced O_3 through the subtropical intrusions within the ASMA region significantly warms around the tropopause region and caused an increase in the UTLS temperature within the ASMA and indirectly leads to the weakening of the ASMA in 2015.

Author contributions: SRB designed the study, conducted research, performed initial data analysis and wrote the first manuscript draft. MVR, GB, SKP and NHL edited the first manuscript. All authors edited the paper.

Data Availability: All the data used in the present study is available freely from the respective websites. The MLS trace gases data obtained from Earth Science Data website. The NCEP/NCAR reanalysis data are available from NOAA website https://www.esrl.noaa.gov/psd/data/gridded/data.ncep.reanalysis.pressure.html). The COSMIC data is available from COSMIC CDAAC website (http://cdaac-www.cosmic.ucar.edu/cdaac/products.html).

Competing interests: The authors declare that they have no conflict of interest.

Acknowledgments: Aura MLS observations obtained from the GES DISC through their FTP site (https://mls.jpl.nasa.gov/index-eos-mls.php) is highly acknowledged. We thank the COSMIC Data Analysis and Archive Centre (CDAAC) for providing RO data used in the present study through their FTP site (http://cdaac-www.cosmic.ucar.edu/cdaac/products.html). We also thank to NCEP/NCAR reanalysis for providing geopotential and wind data. We thank ECMWF for providing ERA interim reanalysis data.

References

Anthes, R., Bernhardt, P., Chen, Y., Cucurull, L., Dymond, K., Ector, D., Healy, S., Ho, S., Hunt, D., Kuo, Y., Liu, H., Manning, K., Mccormick, C., Meehan, T., Randel, W., Rocken, C., Schreiner, W., Sokolovskiy, S., Syndergaard, S., Thompson, D., Trenberth, K., Wee, T., Yen, N., and Zeng, Z.: The COSMIC/FORMOSAT-3 – Mission early results, B. Am. Meteorol. Soc., 89, 313–333, 2008.

Avery, M. A., Davis, S. M., Rosenlof, K. H., Ye, H., Dessler, A. E., 2017. Large anomalies in lower stratospheric water vapour and ice during the 2015–2016 El Niño, Nat. Geosci., 10, 405–409, https://doi.org/10.1038/ngeo2961.

Barnston, A. G. and Livezey, R. E.: Classification, seasonality and persistence of low-frequency atmospheric circulation patterns; Mon. Weather Rev. **115(6)** 1083–1126, 1987.

Basha, G., Ratnam, M. V., and Kishore, P.: Asian Summer Monsoon Anticyclone: Trends and Variability, Atmos. Chem. Phys. Discuss., https://doi.org/10.5194/acp-2019-668, in review, 2019.

Bergman, J. W., Fierli, F., Jensen, E. J., Honomichl, S., and Pan, L. L.: Boundary layer sources for the Asian anticyclone: Regional contributions to a vertical conduit, J. Geophys. Res.-Atmos., 118, 2560–2575, https://doi.org/10.1002/jgrd.50142, 2013.

Bian, J. C., Pan, L. L., Paulik, L., Vömel, H., and Chen, H. B.: In situ water vapor and ozone measurements in Lhasa and Kunming during the Asian summer monsoon, Geophys. Res. Lett., 39, L19808, https://doi.org/10.1029/2012GL052996, 2012.

Braesicke, P., O. J. Smith, P. Telford, and J. A. Pyle (2011), Ozone concentration changes in the Asian summer monsoon anticyclone and lower stratospheric water vapour: An idealised model study, Geophys. Res. Lett., 38, L03810, doi:10.1029/2010GL046228.

Diallo, M., Riese, M., Birner, T., Konopka, P., Müller, R., Hegglin, M. I., Santee, M. L., Baldwin, M., Legras, B., and Ploeger, F.: Response of stratospheric water vapor and ozone to the unusual timing of El Niño and the QBO disruption in 2015–2016, Atmos. Chem. Phys., 18, 13055–13073, https://doi.org/10.5194/acp-18-13055-2018, 2018.

Das, S.S., Suneeth, K.V., Ratnam, M.V., Girach, I. A., Das, S. K.: Upper tropospheric ozone transport from the sub-tropics to tropics over the Indian region during Asian summer monsoon, Clim Dyn., 52: 4567. https://doi.org/10.1007/s00382-018-4418-6, 2019.

Das, S., and Suneeth, K. V.: Seasonal and interannual variations of water vapor in the upper troposphere and lower stratosphere over the Asian Summer Monsoon region- in perspective of the tropopause and ocean-atmosphere interactions", Journal of Atmospheric and Solar-Terrestrial Physics 201, 105244, doi:10.1016/j.jastp.2020.105244, 2020.

Dessler, A. E., Schoeberl, M. R., Wang, T., Davis, S. M., Rosenlof, K. H., and Vernier, J. P.: Variations of stratospheric water vapor over the past three decades, J. Geophys. Res. Atmos., 119, 12 588–12 598, doi:10.1002/2014JD021712, 2014.

Dunkerton, T. J.: The quasi-biennial oscillation of 2015–2016: Hiccup or death spiral?, Geophys. Res. Lett., 43, 10547–10552, https://doi.org/10.1002/2016GL070921, 2016.

Fadnavis, S. and Chattopadhyay, R.: Linkages of subtropical stratospheric intraseasonal intrusions with Indian summer monsoon deficit rainfall, J. Climate, 30, 5083–5095, https://doi.org/10.1175/JCLI-D-16-0463.1, 2017.

Fadnavis, S., Sabin, T.P., Roy, C. et al.: Elevated aerosol layer over South Asia worsens the Indian droughts. Sci Rep 9, 10268, doi:10.1038/s41598-019-46704-9, 2019.

Fan, Q., Bian, J. and Pan, L. L.: Stratospheric entry point for upper-tropospheric air within the Asian summer monsoon anticyclone, Sci. China Earth Sci., 60, 1685–1693, https://doi.org/10.1007/s11430-016-9073-5, 2017.

Fishman, J., and Seiler, W.: Correlative nature of ozone and carbon monoxide in the troposphere - Implications for the tropospheric ozone budget; J. Geophys. Res. 88, https://doi.org/10.1029/JC088iC06p03662, 1983.

https://doi.org/10.5194/acp-2020-1075
Preprint. Discussion started: 16 November 2020

Fueglistaler, S., Dessler, A. E., Dunkerton, T. J., Folkins, I., Fu, Q., and Mote, P. W.: Tropical Tropopause Layer, Rev. Geophys., 47, G1004+, https://doi.org/10.1029/2008RG000267, 2009.

Gadgil, S. and Francis, P. A.: El Niño and the Indian rainfall in June. Curr Sci 110:1010–1022, 2016.

Garny, H. and Randel, W. J.: Transport pathways from the Asian monsoon anticyclone to the stratosphere, Atmos. Chem. Phys., 16, 2703–2718, https://doi.org/10.5194/acp-16-2703- 2016, 2016.

Gettelman, A., Randel, W. J., Massie, S., Wu, F.: El Niño as a natural experiment for studying the tropical tropopause region, J. Clim., 14, 3375– 3392, 2001.

Gettelman, A., Kinnison, D. E., Dunkerton, T. J., and Brasseur, G. P.: Impact of monsoon circulations on the upper troposphere and lower stratosphere, J. Geophys. Res.-Atmos., 109, D22101, https://doi.org/10.1029/2004JD004878, 2004.

Highwood, E. J. and Hoskins, B. J.: The tropical tropopause, Q. J. Roy. Meteor. Soc., 124, 1579–1604, https://doi.org/10.1002/qj.49712454911, 1998.

Ho, S.-P., Anthes, R. A., Ao, C.O., Healy, S., Horanyi, A., Hunt, D., Mannucci, A.J., Pedatella, N., Randel, W.J., Simmons, A., Steiner, A., Xie, F., Yue, X., Zeng., Z.: The COSMIC/FORMOSAT-3 radio occultation mission after 12 years: Accomplishments, remaining challenges, and potential impacts of COSMIC-2. Bull Amer Met Soc 100 online version: https://journals.ametsoc.org/doi/pdf/10.1175/BAMS-D-18-0290.1

Honomichl, S. B., and Pan, L. L.: Transport from the Asian summer monsoon anticyclone over the western Pacific. Journal of Geophysical Research: Atmospheres, 125, e2019JD032094. https://doi.org/10.1029/2019JD032094, 2020.

Jain, S., and Kar, S.C.: Transport of water vapour over the Tibetan Plateau as inferred from the model simulations. J. Atmos. Sol. Terr. Phys. 161, 64–75. https://doi.org/ 10.1016/j.jastp.2017.06.016, 2017.

Jiang, J.H., Su, H., Zhai, C., Wu, L., Minschwaner, K., Molod, A.M., Tompkins, A.M.: An assessment of upper troposphere and lower stratosphere water vapor in MERRA, MERRA2, and ECMWF reanalyses using Aura MLS observations. J. Geophys. Res. Atmos. 120, 11. https://doi.org/10.1002/2015JD023752, 468–11,485, 2015.

Kalnay, E., Kanamitsu, M., Kistler, R., Collins, W., Deaven, D., Gandin, L., Iredell, M., Saha, S., White, G., Woollen, J., Zhu, Y., Leetmaa, A., Reynolds, R., Chelliah, M., Ebisuzaki, W.,

https://doi.org/10.5194/acp-2020-1075
Preprint. Discussion started: 16 November 2020

Atmospheric Chemistry and Physics Discussions

Higgins, W., Janowiak, J., Mo, K. C., Ropelewski, C., Wang, J., Jenne, R., and Joseph, D.: The NCEP/NCAR 40 year reanalysis project, B. Am. Meteorol. Soc., 77, 437–471, 1996.

Khan, A., Jin, S.: Effect of gravity waves on the tropopause temperature, altitude and water vapor in Tibet from COSMIC GPS Radio Occultation observations, J. Atmos. Sol. Terr. Phys. 138–139, 23–31. https://doi.org/10.1016/j.jastp.2015.12.001, 2016.

Kim, J. and Son, S.-W.: Tropical Cold-Point Tropopause: Climatology, Seasonal Cycle, and Intraseasonal Variability Derived from COSMIC GPS Radio Occultation Measurements, J. Climate, 25, 5343–5360, https://doi.org/10.1175/JCLI-D-11-00554.1, 2012.

Kumar, K. K., Rajagopalan, B., Cane, M. A.: On the weakening relationship between the Indian monsoon and ENSO. Science 287:2156–2159, 1999.

Kunze, M., Braesicke, P., Langematz, U., Stiller, G., Bekki, S., Brühl, C., Chipperfield, M., Dameris, M., Garcia, R., and Giorgetta, M.: Influences of the Indian Summer Monsoon on Water Vapor and Ozone Concentrations in the UTLS as Simulated by Chemistry–Climate Models, J. Climate, 23, 3525–3544, https://doi.org/10.1175/2010jcli3280.1, 2010.

Kursinski, E. R., Hajj, G. A., Schofield, J. T., Linfield, R. P., and Hardy, K. R.: Observing Earth's atmosphere with radio occultation measurements using the Global Positioning System, J. Geophys. Res., 102, 23429–23465, 1997.

Li, Q., Jiang, J. H., Wu, D. L., Read, W. G., Livesey, N. J., Waters, J. W., Zhang, Y., Wang,B., Filipiak, M. J., Davis, C. P., Turquety, S., Wu, S., Park, R. J., Yantosca, R. M., and Jacob, D. J.: Convective outflow of South Asian pollution: A global CTM simulation compared with EOS MLS observations, Geophys. Res. Lett., 32, L14 826, https://doi.org/10.1029/2005GL022762, 2005.

Li J, Yu. R. and Zhou, T.: Teleconnection between NAO and climate downstream of the Tibetan Plateau; J. Climate **21(18),** 4680–4690, 2008.

Li, D. and Bian, J.: Observation of a Summer Tropopause Fold by Ozonesonde at Changchun, China: Comparison with Reanalysis and Model Simulation, Adv. Atmos. Sci., 32, 1354–1364, https://doi.org/10.1007/s00376-015-5022-x, 2015.

Li, D., Vogel, B., Müller, R., Bian, J., Günther, G., Li, Q., Zhang, J., Bai, Z., Vömel, H., and Riese, M.: High tropospheric ozone in Lhasa within the Asian summer monsoon anticyclone in 2013: influence of convective transport and stratospheric intrusions, Atmospheric Chemistry and

https://doi.org/10.5194/acp-2020-1075
Preprint. Discussion started: 16 November 2020

Atmospheric Chemistry and Physics Discussions

Physics, 18, 17 979–17 994, https://doi.org/10.5194/acp-18-17979-2018, https://www.atmos-chem-phys.net/18/17979/2018/, 2018.

Lin, Z.D. and Lu, R. Y.: Inter annual meridional displacement of the East Asian upper-tropospheric jet stream in summer. Advances in Atmospheric Sciences, 22, 199– 211, 2005.

Livesey, N. J., Read, W. G., Wagner, P. A., Froidevaux, L., Lambert, A., Manney, G. L., Valle, L. F. M., Pumphrey, H. C., Santee, M. L., Schwartz, M. J., Wang, S., Fuller, R. A., Jarnot, R. F., Knosp, B. W., and Martinez, E.: Version 4.2x Level 2 data quality and description document, https://mls.jpl.nasa.gov/data/v4-2_data_quality_document.pdf, 2018

Nützel, M., Dameris, M., and Garny, H.: Movement, drivers and bimodality of the South Asian High, Atmos. Chem. Phys., 16, 14755–14774, https://doi.org/10.5194/acp-16-14755-2016, 2016.

Pan, L. L., Honomichl, S. B., Kinnison, D. E., Abalos, M., Randel, W. J., Bergman, J. W., and Bian, J. C.: Transport of chemical tracers from the boundary layer to stratosphere associated with the dynamics of the Asian summer monsoon, J. Geophys. Res.-Atmos., 121, 14159–14174, https://doi.org/10.1002/2016JD025616, 2016.

Park, M., Randel, W. J., Kinnison, D. E., Garcia, R. R., and Choi, W.: Seasonal variation of methane, water vapor, and nitrogen oxides near the tropopause: Satellite observations and model simulations, J. Geophys. Res.-Atmos., 109, D03302, https://doi.org/10.1029/2003jd003706, 2004.

Park, M., Randel, W. J., Gettelman, A., Massie, S. T., and Jiang, J. H.: Transport above the Asian summer monsoon anticyclone inferred from Aura MLS tracers, J. Geophys. Res, 112, D16309, doi:10.1029/2006JD008294, 2007.

Park, M., Randel, W. J., Emmons, L. K., Bernath, P. F., Walker, K. A., and Boone, C. D.: Chemical isolation in the Asian monsoon anticyclone observed in Atmospheric Chemistry Experiment (ACE-FTS) data, Atmos. Chem. Phys., 8, 757–764, https://doi.org/10.5194/acp-8-757-2008, 2008

Park, M., Randel, W. J., Emmons, L. K., and Livesey, N. J.: Transport pathways of carbon monoxide in the Asian summer monsoon diagnosed from Model of Ozone and Related Tracers (MOZART), J. Geophys. Res., 114, D08303, https://doi.org/10.1029/2008JD010621, 2009.

Ramaswamy, C.: A preliminary study of the behavior of the Indian southwest monsoon in relation to the westerly jet-stream. Special Palmen No. Geophysica, 6, pp. 455-476, 1958.

Randel, W. J. and Park, M.: Deep convective influence on the Asian summer monsoon anticyclone and associated tracer variability observed with Atmospheric Infrared Sounder (AIRS), J. Geophys. Res., 111, D12314, https://doi.org/10.1029/2005jd006490, 2006.

Randel, W. J., Park, M., Emmons, L., Kinnison, D., Bernath, P., Walker, K. A., Boone, C., and Pumphrey, H.: Asian monsoon transport of trace gases to the stratosphere, Science, 328, 611–613, 10.1126/science.1182274, 2010.

Randel, W. J., Park, M., Emmons, L., Kinnison, D., Bernath, P., Walker, K. A., Boone, C., and Pumphrey, H.: Asian Monsoon Transport of Pollution to the Stratosphere, Science, 328, 611–613, https://doi.org/10.1126/science.1182274, 2010.

Rao, D.N., Ratnam, M.V., Mehta, S., Nath, D., Basha, G., Jagannadha Rao, V.V.M., et al: Validation of the COSMIC radio occultation data over gadanki (13. 48°N, 79.2°E): A tropical region, Terr J Atmos Ocean Sci 20, 59–70, https://doi.org/10.3319/TAO.2008.01.23.01(F3C), 2009.

RavindraBabu, S., VenkatRatnam, M., Basha, G., Krishnamurthy, B. V., and Venkateswararao, B.: Effect of tropical cyclones on the tropical tropopause parameters observed using COSMIC GPS RO data, Atmos. Chem. Phys., 15, 10239–10249, doi:10.5194/acp-15-10239-2015, 2015.

RavindraBabu, S., VenkataRatnam, M., Basha, G., Liou, Y.-A., Narendra Reddy, N.: Large Anomalies in the Tropical Upper Troposphere Lower Stratosphere (UTLS) Trace Gases Observed during the Extreme 2015–16 El Niño Event by Using Satellite Measurements, Remote Sensing. 2019, 11, 687.https://doi.org/10.3390/rs11060687, 2019. a

RavindraBabu, S., Venkat Ratnam, M., Basha, G., Krishnamurthy, B.V.: Indian summer monsoon onset signatures on the tropical tropopause layer. Atmos. Sci. Lett. 20, e884. https://doi.org/10.1002/asl.884, 2019. b

Ravindra Babu, S., Akhil Raj, S.T., Basha, G., Venkat Ratnam, M.: Recent trends in the UTLS temperature and tropical tropopause parameters over tropical South Indian region, J. Atmos. Solar Terr.Phys. 197:105164. https://doi.org/10.1016/j.jastp.2019.105164, 2020.

Samanta, D., Dash, M. K., Goswami, B. N., and Pandey, P. C.: Extratropical anticyclonic Rossby wave breaking and Indian summer monsoon failure. Climate Dyn., 46, 1547–1562, doi:https://doi.org/10.1007/s00382-015-2661-7., 2016.

Santee, M. L., Manney, G. L., Livesey, N. J., Schwartz, M. J., Neu, J. L., and Read, W. G.: A comprehensive overview of the climatological composition of the Asian summer monsoon

https://doi.org/10.5194/acp-2020-1075
Preprint. Discussion started: 16 November 2020

Atmospheric Chemistry and Physics
Discussions

anticyclone based on 10 years of Aura Microwave Limb Sounder measurements, J. Geophys. Res.-Atmos., 122, 5491- 5514, https://doi.org/10.1002/2016jd026408, 2017.

Scherllin-Pirscher, B., Kirchengast, G., Steiner, A. K., Kuo, Y.-H., and Foelsche, U.: Quantifying uncertainty in climatological fields from GPS radio occultation: an empirical-analytical error model, Atmos. Meas. Tech., 4, 2019–2034, doi:10.5194/amt-4-2019-2011, 2011a.

Scherllin-Pirscher, B., Steiner, A. K., Kirchengast, G., Kuo, Y.-H., and Foelsche, U.: Empirical analysis and modeling of errors of atmospheric profiles from GPS radio occultation, Atmos. Meas. Tech., 4, 1875–1890, doi:10.5194/amt-4-1875-2011, 2011b.

Shine, K. P. and Forster, P. M. D. F.: The effect of human activity on radiative forcing of climate change: a review of recent developments, Glob. Planet. Change, 20, 205–225, 1999.

Song, Y., Lü, D., Li, Q., Bian, J., Wu, X., and Li, D.: The impact of cut-off lows on ozone in the upper troposphere and lower stratosphere over Changchun from ozonesonde observations, Adv. Atmos. Sci., 33, 135–150, https://doi.org/10.1007/s00376-015- 5054-2, 2016.

Sprenger, M., Maspoli, M. C., and Wernli, H.: Tropopause folds and cross-tropopause exchange: A global investigation based upon ECMWF analyses for the time period March 2000 to February 2001, J. Geophys. Res., 108, 8518, https://doi.org/10.1029/2002JD002587, 2003.

Škerlak, B., Sprenger, M., and Wernli, H.: A global climatology of stratosphere–troposphere exchange using the ERA-Interim data set from 1979 to 2011, Atmos. Chem. Phys., 14, 913–937, https://doi.org/10.5194/acp-14-913-2014, 2014.

Tweedy, O. V., Waugh, D. W., Randel, W. J., Abalos, M., Oman, L. D., and Kinnison, D. E.: The Impact of Boreal Summer ENSO Events on Tropical Lower Stratospheric Ozone, Journal of Geophysical Research: Atmospheres, 123, 9843–9857, https://doi.org/10.1029/2018JD029020.

Uppala, S. M., Kållberg, P. W., Simmons, A. J., Andrae, U., da Costa Bechtold, V., Fiorino, M., Gibson, J. K., Haseler, J., Hernandez, A., Kelly, G. A., Li, X., Onogi, K., Saarinen, S., Sokka, N., Allan, R. P., Andersson, E., Arpe, K., Balmaseda, M. A., Beljaars, A. C. M., van de Berg, L., Bidlot, J., Bormann, N., Caires, S., Chevallier, F., Dethof, A., Dragosavac, M., Fisher, M., Fuentes, M., Hagemann, S., Hólm, E., Hoskins, B. J., Isaksen, L., Janssen, P. A. E. M., Jenne, R., McNally, A. P., Mahfouf, J. F., Morcrette, J. J., Rayner, N. A., Saunders, R. W., Simon, P., Sterl, A., Trenberth, K. E., Untch, A., Vasiljevic, D., Viterbo, P., and Woollen, J.: The ERA-40 re-analysis, Q. J. Roy. Meteor. Soc., 131, 2961–3012, https://doi.org/10.1256/qj.04.176, 2005.

Vellore, R. K., Kaplan, M. L., and Krishnan, R., et al.: Monsoon-extratropical circulation interactions in Himalayan extreme rainfall; *Clim. Dyn.* **46,** 3517, 2016. https://doi.org/10.1007/s00382-015-2784-x.

Venkat Ratnam, M., Ravindra Babu, S., Das, S. S., Basha, G., Krishnamurthy, B. V., and Venkateswararao, B.: Effect of tropical cyclones on the stratosphere–troposphere exchange observed using satellite observations over the north Indian Ocean, Atmos. Chem. Phys., 16, 8581–8591, https://doi.org/10.5194/acp-16-8581-2016, 2016.

Vernier, J.-P., Thomason, L. W., and Kar, J.: CALIPSO detection of an Asian tropopause aerosol layer, Geophys. Res. Lett., 38, L07804, https://doi.org/10.1029/2010GL046614, 2011

Vernier, J.-P., Fairlie, T. D., Deshler, T., Ratnam, M. V., Gadhavi, H., Kumar, B. S., Natarajan, M., Pandit, A. K., Raj, S. T. A., Kumar, A. H., Jayaraman, A., Singh, A. K., Rastogi, N., Sinha, P. R., Kumar, S., Tiwari, S., Wegner, T., Baker, N., Vignelles, D., Stenchikov, G., Shevchenko, I., Smith, J., Bedka, K., Kesarkar, A., Singh, V., Bhate, J., Ravikiran, V., Rao, M. D., Ravindrababu, S., Patel, A., Vernier, H., Wienhold, F. G., Liu, H., Knepp, T. N., Thomason, L., Crawford, J., Ziemba, L., Moore, J., Crumeyrolle, S., Williamson, M., Berthet, G., Jégou, F., and Renard, J.- B.: BATAL: The balloon measurement campaigns of the Asian tropopause aerosol layer, B. Am. Meteorol. Soc., 99, 955–973, https://doi.org/10.1175/BAMS-D-17-0014.1, 2018.

Vogel, B., Günther, G., Müller, R., Grooß, J.-U., Afchine, A., Bozem, H., Hoor, P., Krämer, M., Müller, S., Riese, M., Rolf, C., Spelten, N., Stiller, G. P., Ungermann, J., and Zahn, A.: Longrange transport pathways of tropospheric source gases originating in Asia into the northern lower stratosphere during the Asian monsoon season 2012, Atmos. Chem. Phys., 16, 15301–15325, https://doi.org/10.5194/acp-16-15301-2016, 2016.

Wang, B., Xiang, B., Li, J., Webster, P. J., Rajeevan, M. N., Liu, J., Ha, K. –J.: Rethinking Indian monsoon rainfall prediction in the context of recent global warming. Nat Commun 6:7154. doi:10.1038/ncomms8154, 2015.

Xu, X., Zhao, T., Lu, C., Guo, Y., Chen, B., Liu, R., Li, Y., Shi, X.: An important mechanism sustaining the atmospheric "water tower" over the Tibetan Plateau. Atmos. Chem. Phys. 14, 11287–11295. https://doi.org/10.5194/acp-14-11287- 2014.

Yan, R.-C., Bian, J.-C., and Fan, Q.-J.: The Impact of the South Asia High Bimodality on the Chemical Composition of the Upper Troposphere and Lower Stratosphere, Atmos. Ocean. Sci.

https://doi.org/10.5194/acp-2020-1075
Preprint. Discussion started: 16 November 2020

Lett., 4, 229–234, 2011.

Yan, R. C. and Bian, J. C.: Tracing the boundary layer sources of carbon monoxide in the Asian summer monsoon anticyclone using WRF–Chem, Adv. Atmos. Sci., 32, 943–951, https://doi.org/10.1007/s00376-014-4130-3, 2015.

Yan, X., Konopka, P., Ploeger, F., Tao, M., Müller, R., Santee, M. L., Bian, J., and Riese, M.: El Niño Southern Oscillation influence on the Asian summer monsoon anticyclone, Atmospheric Chemistry and Physics, pp. 8079–8096, https://doi.org/10.5194/acp-18-8079-2018, 2018.

Yang, S., Lau, K.-M., Yoo, S.-H., Kinter, J. L., Miyakoda, K. and Ho, C.-H.: Upstream subtropical signals preceding the Asian summer monsoon circulation; J. Climate, 17, 4213–4229, 2004.

Yu, P., Rosenlof, K. H., Liu, S., Telg, H., Thornberry, T. D., Rollins, A. W., Portmann, R. W., Bai, Z., Ray, E. A., Duan, Y., Pan, L. L., Toon, O. B., Bian, J., and Gao, R.-S.: Efficient transport of tropospheric aerosol into the stratosphere via the Asian summer monsoon anticyclone, Proceedings of the National Academy of Sciences, pp. 6972–6977, https://doi.org/10.1073/pnas.1701170114, 2017.

Yuan, C., Lau, W. K. M., Li, Z., and Cribb, M.: Relationship between Asian monsoon strength and transport of surface aerosols to the Asian Tropopause Aerosol Layer (ATAL): interannual variability and decadal changes, Atmos. Chem. Phys., 19, 1901-1913, https://doi.org/10.5194/acp-19-1901-2019, 2019.

Zhang, Q., Wu, G., and Qian, Y.: The Bimodality of the 100 hPa South Asia High and its Relationship to the Climate Anomaly over East Asia in Summer, J. Meteorol. Soc. Jpn., 80, 733–744, 2002.

Zheng, B., Chevallier, F., Ciais, P., Yin, Y., Deeter, M. N., Worden, H. M., Wang, Y., Zhang, Q., and He, K.: Rapid decline in carbon monoxide emissions and export from East Asia between years 2005 and 2016, Environ. Res. Lett., 13, 044007, https://doi.org/10.1088/1748-9326/aab2b3, 2018.